University of La Laguna

Master's Degree in Renewable Energy

2021/2022

Master Thesis

Development and Evaluation of Open-Source prEN50549-10 Tests Scripts for Improved Solar Integration

September 4, 2022

Author: Fouad Jose Salazar Hamze

Advisors: Ricardo Guerrero Lemus[1] & Roland Bründlinger[2]

[1]ULL University of La Laguna, Department of Applied Physics
[2]AIT Austrian Institute of Technology, Center for Energy

Abstract

Distributed Energy Resources (DERs), such as Photovoltaic (PV) inverters, have the capability to provide a range of services for power system operators. The prEN50549-10 draft standard, which outlines test procedures for the grid support functions of the DER, is an essential tool to certify that PV inverters comply with the stated functions. Open-Source prEN50549-10 Python Tests Scripts that automatically execute test procedures for the certification standard are developed and evaluated in this study. For that purpose, a Controller Hardware-In-The-Loop (CHIL) testbed integrated with automated testing was used. The system comprises a 34.5 kW Austrian Institute of Technology (AIT) Smart Grid Converter (SGC) connected to a Typhoon HIL 402 system, and the evaluations for the automation of grid support function tests rely on the SunSpec System Validation Platform (SVP) to execute sequences of testing logic that change settings on the Device Under Test (DUT), grid simulator, PV simulator, and data acquisition system using Python scripts. As a result, it was obtained for the first time Python Test Scripts that allow the automatic execution of the certification test for the grid support functions of "Active response to frequency deviation", "Voltage support by reactive power", and "Voltage related to active power reduction" as stated in the prEN50549-10 standard.

Contents

List of Figures

List of Tables

1 Introduction

The worldwide use of photovoltaic energy is constantly increasing in such a way that studies carried out by the International Energy Agency (IEA) state that the average annual generation growth is estimated to be around 24% between 2020 and 2030, which corresponds to 630 GW of net capacity additions in 2030 [1]. This worldwide capacity growth brings an increasing penetration of inverter-based renewable energy resources on electrical grids. Therefore, grid support functions have been developed on Distributed Energy Resources (DERs), such as photovoltaic (PV) inverters, to positively influence power systems by providing voltage and frequency support to respond to the grid during a fault.

Different standards have been developed in each country to meet the tests and evaluations required to certify that the grid support functions of equipment and systems are regulated under the network codes as needed. In the USA, IEEE 1547.1 standard defines requirements for interconnection and grid-support functions for DER devices, and therefore American and Canadian PV inverter certifications are currently conducted based on UL 1741 which references IEEE 1547.1 [2]. In Europe, the prEN50549-10, which currently is a draft standard, provides technical guidance for tests on generating units and interface protection to evaluate their electrical characteristics, aiming to demonstrate the conformity of generating units to technical requirements for grid connection [3].

To evaluate compliance of grid support functions according to each standard, Controller Hardware-In-The-Loop (CHIL) is a powerful tool that performs real-time simulation for embedded control systems and has the flexibility to easily operate for a range of systems, control schemes, and grid conditions, and unlike other certification methods, eliminates power requirements making it easier to test full-scale equipment as power electronics devices continue to grow to megawatt-scale [4]. Therefore, CHIL is slowly becoming an alternative to power system testing for certification standards, and this tool can be even more powerful when automation of the processes involved can be achieved. Some studies [2, 4, 5], have shown the importance of automating the certification process according to IEEE 1547.1 standard, emphasizing that these processes are highly detailed with specifications for measurement and test equipment accuracy, and include a high amount of measurement points for the grid-support functions, making the automation a necessity. However, despite the studies carried out to automate the certification processes proposed in the IEEE 1547.1 standard, there is no research on the automation of the certification process in the prEN50549-10 standard. Therefore this study aims to develop an Open-Source prEN50549-10 Python Tests Scripts that automatically executes test

procedures for the certification standard.

The testbed of the study is conformed by a 34.5 kW Austrian Institute of Technology (AIT) smart grid converter (SGC) connected to a Typhoon HIL 402 system. This CHIL system relies on the SunSpec System Validation Platform (SVP) to perform the automation of grid support function. The SVP allows the communication with the HIL simulator and with the Equipment Under Test (EUT), which for this study is refered to the PV Inverter controller, and through the employment of Python Test Scripts different sequences of testing logic are performed by changing settings on the DUT, grid simulator, PV simulator, and data acquisition system. In this way, this study provides the test scripts to perform the automation of the certification procedure for the following grid support functions stated in the prEN50549-10 standard:

- Active response to frequency deviation.
- Voltage support by reactive power.
- Voltage related to active power reduction.

The resulting automation of the certification procedure for the mentioned functions is expected to provide significant benefits over traditional power laboratory testing by validating the grid support functions of PV inverters without complex and expensive power laboratory equipment, and also by providing an Open-Source SVP repository with Python Test Scripts necessary to verify the controller's performance before hardware integration. It is important to emphasize that this study is based on the existing Open-Source SVP repository for the evaluation of the grid support function of the IEEE 1547.1 standard, and the main objective is the development of a new repository in which the necessary scripts for the evaluation according to the prEN50549-10 standard can be integrated. Hence, a literature review, the methodology used for the development of the new Open-Source SVP repository, and subsequent evaluation of the results obtained, are presented in the next sections.

2 Literature Review

This section aims to provide a literature review, mainly based on papers, conference proceedings, publications on recognized websites, and books to define the concepts required to perform the test automation of the grid support functions specified in prEN50549-10.

2.1 Distributed Energy Resources

Distributed Energy Resources (DER) refers to electric power generation resources that are directly connected to medium voltage (MV) or low voltage (LV) distribution systems, rather than to the bulk power transmission systems [6]. DERs include a wide range of electrical energy technologies such as distributed generators, renewable energy resources, and energy storage systems [7]. The categorization of the technologies that DERs involves can be summarized as proposed in Fig. 1.

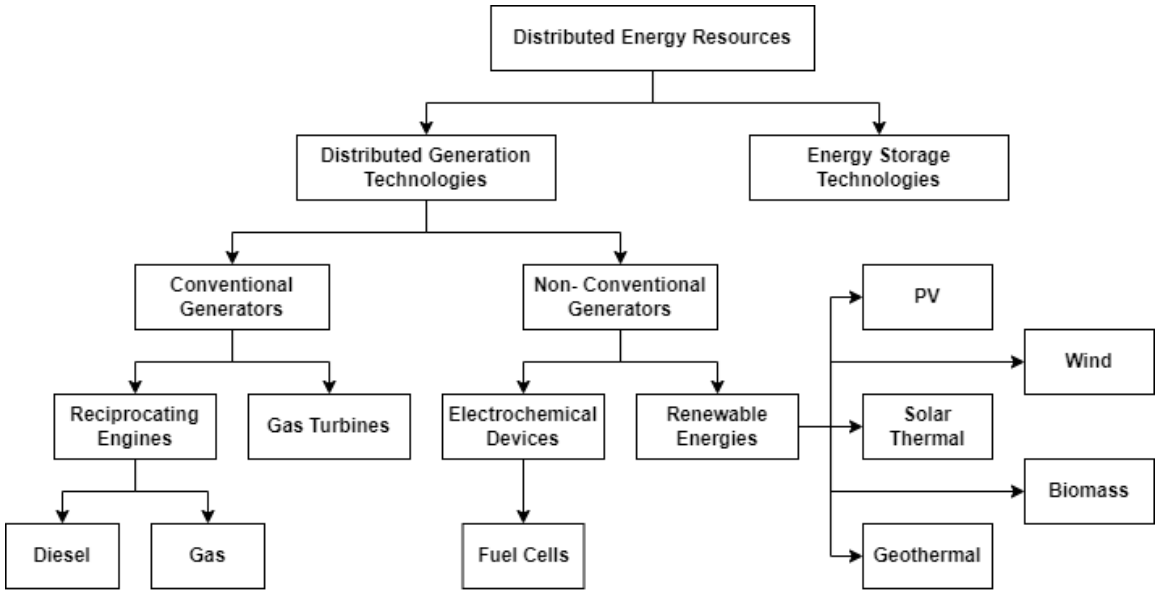

Figure 1: Distributed Energy Resources Technologies. Adapted from [6].

As is shown in Fig. 1, DERs are primarily divided into Distributed Generation (DG) and Energy Storage Technologies. The definition of DG Technologies varies according to the sources and capacities, but can be generally defined as any source of electric power of limited capacity, directly connected to the power system distribution network where it is consumed by the end users, and on the other hand, energy storage is generally defined as the conversion process from electrical energy to another form of potential energy [6].

2.2 Photovoltaic Systems

According to [8], Photovoltaic (PV) systems are a type of Non-Conventional generators technology of the DER that consists of PV modules, which are discrete multiple cells, connected either in series or parallel, that convert solar radiation into electricity. A typical PV system comprises a PV module or modules, batteries, and an inverter, and could be stand-alone or connected to the grid. Stand-alone PV systems are used in areas that are not easily accessible or have no access to an electric grid, therefore this kind of PV system is independent of the electricity grid, with the energy produced normally being stored in batteries [8]. On the other hand, the PV systems connected to the grid, which are interest of in this study, are systems connected to the local electricity network using inverters as shown in Fig. 2. Currently, grid-connected PV systems are a usual practice, and considering its significant expansion, the design and operation of power converters is crucial to achieve high efficiency for different power configurations and grid support functions. Consequently, the performance of the PV inverters connected to the grid is considered key to improve solar integration and is discussed in the next sections.

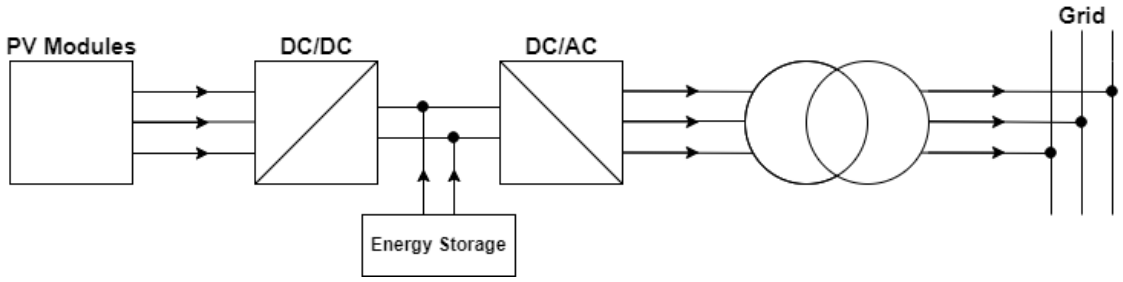

Figure 2: Grid-Connected PV System schematic diagram. Adapted from [8].

2.3 PV Inverter

A PV inverter is a kind of electronic circuit for energy conversion, which converts electrical energy of the supply into the energy suitable for the load, in other words, a PV inverter converts Direct Current (DC) power to Altern Current (AC) power. The AC outputs after the DC-to-AC inversion can be single phase or multiphase, and most common waveforms of the outputs of the inverters are square wave, sinusoidal wave, or modified sinusoidal wave [9]. This study focuses on the three phase voltage-source inverters, which configuration and topology is shown in Fig. 3. The PV inverters have techniques that can regulate the output AC voltage with suitable amplitudes and frequencies, it can also reduce the harmonics by implementing multiple switching within the inverter with a constant DC input voltage [9]. Therefore, in case of abnormal grid conditions and faults, the inverters no longer have to disconnect and wait for fault

clearance. This is essential considering that the massive development in the PV sector faced new challenges for the inverters that are now required to contribute to grid stability by providing grid support.

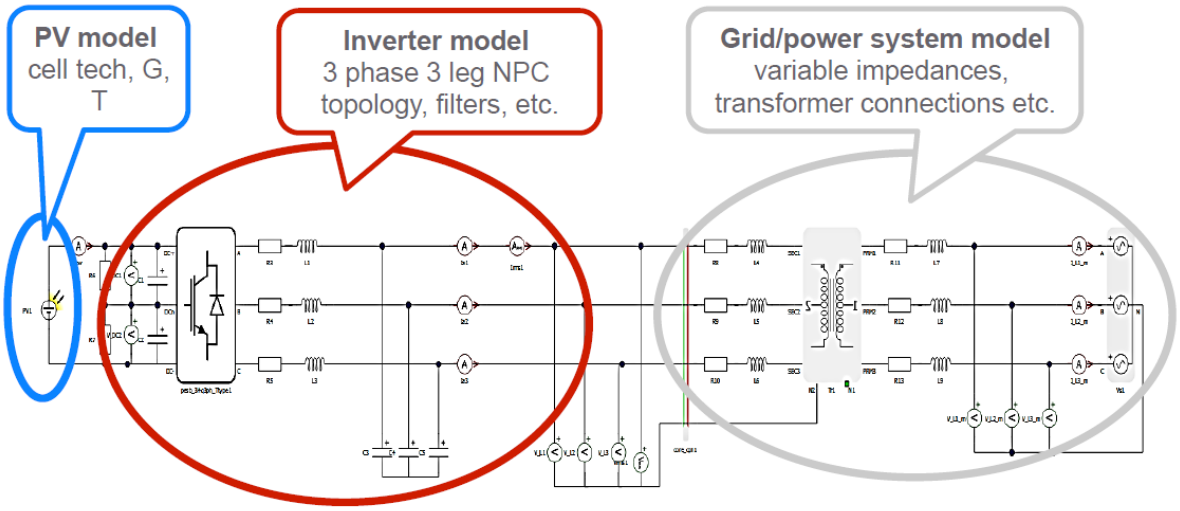

Figure 3: AIT Three Phase Voltage-Source Inverter Topology. Adapted from [10].

2.4 Grid Support Functions of the PV Inverters

A fast increase of DERs in electrical grids may cause negative impacts on the distribution networks that were not designed to host a high share of DG in the LV and MV networks. The variation in energy production from renewable energy resources may cause, among other events, the fluctuation in voltage profiles, congestions, bi-directional power flows, poor reliability, and an increase in distribution costs [11]. The voltage fluctuation is one of the most important concerns for active distribution networks, and results as the consequence of an excessive load or generation, in such a way that when the network suffers a low load with high generation occurs an over-voltage, and when it suffers a high load with low generation occurs an under-voltage [12]. In Fig. 4 a scheme that simplifies the effects of the elements connected to the point of common coupling (PCC) on the grid voltage is presented.

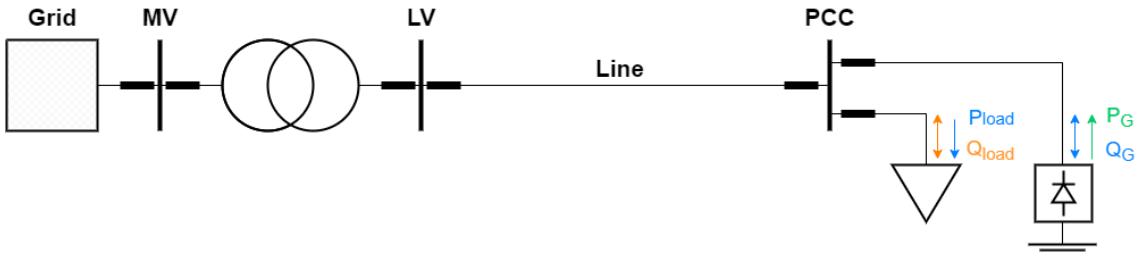

Figure 4: Elements connected to the PCC on the grid voltage. Adapted from [13].

To understand the impact of load and generation on the voltage profile of a simple distribution line, note that the load consumes active power from the grid (P_{load}) and causes a voltage drop over the line that may lead to low grid voltages at the PCC. If the type of load is inductive or capacitive, it can either absorb or inject reactive power (Q_{load}). When DERs inject active power (P_G) into the grid, it can cause a voltage rise over the line and may lead to high voltages at the PCC [13]. Therefore, in the cases when voltage at PCC exceeds the permissible voltage level, DERs must be able to take action to address the voltage range permitted.

The conventional ways to regulate distribution voltages are on-load tap-changing transformers, also known as voltage regulators, and capacitor banks, and even though the use of these methods has been a common practice for decades, they lack the flexibility to face the challenges of the new active distribution networks where fast responses to ramping behavior of solar PV are needed [12]. This is where the PV inverters take place, and by using voltage control strategies can contribute to maintaining the voltage at their PCC within permitted levels. To understand how voltage support of PV Inverter works, an equivalent circuit of the grid, from the generator perspective, is presented in Fig. 5.

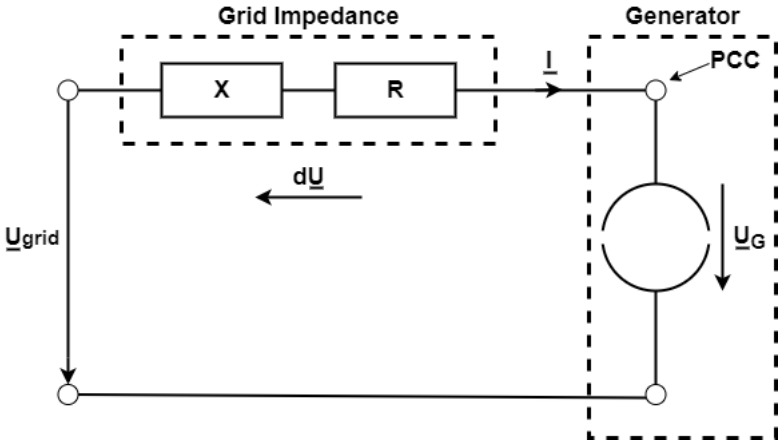

Figure 5: Schematic of a generator connected to a grid section. Adapted from [14].

To estimate the specific voltage deviation (dU) over the grid impedance, Eq. 1 is proposed [14], which demonstrates the relationship between grid resistance (R), grid reactance (X), active power of the generator (P), and reactive power of the generator (Q). From this approximation, it is noted that the PCC voltage rises by increasing the active power feed-in, while the reactive power can either reduce the voltage (inductive consumption, under-excited) or increase the voltage (capacitive consumption, over-excited).

$$dU \approx \frac{(R \cdot P) + (\mp Q \cdot X)}{(U_{\text{Grid}})^2} \tag{1}$$

However, it must be considered that reactive power control for a certain generator phase angle depends on the R/X characteristics of the respective grid section. By fixing Eq. 1, and setting it as a function of the generator phase angle (φ), Eq. 2 is obtained, which shows that the larger the R/X ratio, the more reactive power is needed to compensate the voltage increase.

$$dU \approx \frac{R \cdot P}{(U_{\text{Grid}})^2} \cdot \left[1 + \tan\varphi \cdot \frac{1}{R/X}\right] \tag{2}$$

This is especially relevant when considering using grid support functions of the PV inverters, since the impact of PV active and reactive power variations on the grid voltage depends strongly on the electrical characteristics (especially R/X ratio) of each grid node.

2.5 prEN50549-10

The prEN50549-10, which is currently a draft, is an European Standard that aims to provide technical guidance for tests on generating units and interface protection to evaluate their electrical characteristics [3]. The requirements evaluated on this standard are covered in:

- EN 50549-1:2019: Requirements for generating plants to be connected in parallel with distribution networks - Part 1: connection to a LV distribution network - Generating plants up to and including Type B [15].
- EN 50549-2:2019: Requirements for generating plants to be connected in parallel with distribution networks - Part 2: Connection to a MV distribution network - Generating plants up to and including Type B [16].

This study focuses on section 5 of the prEN50549-10 standard regarding the testing of grid support functions of the PV inverters. In accordance with the requirements of section 4.2.1 related to testing complete generating units, tests must be performed on an EUT covering the complete generating unit from the primary energy converter, and the nominal frequency and voltage of the outputs of the EUT corresponds to the nominal values of the LV distribution network. For more details about the testing conditions that are specified in prEN50549-10, please refer to the annexes section.

2.5.1 Active response to frequency deviation

The prEN50549-10 defines in the section 5.4 test procedures related to the capability of generating units to respond to frequency changes. It is stated that generating plants shall be capable of activating active power response to over-frequency and under-frequency at a programmable frequency threshold $f1$ with a programmable droop in a range of at least s=2% to s=12%. From the EN50549-1:2019 standard [15], Eq. 3 is used to set the required setting of the change in the active power (ΔP) injected by the inverter as a function of the grid frequency (f), the frequency threshold ($f1$), the nominal frequency of the grid (f_n), and the programmable droop (s).

$$\Delta P = \frac{1}{s} \cdot \frac{(f_1 - f)}{f_n} \cdot P_{ref} \tag{3}$$

Fig. 6 shows an example of the inverter response to grid over-frequency. On the left panel is presented how the response should be when f_{stop} command is deactivated, that means that the active power frequency response is only deactivated if the frequency falls below $f1$. On the other hand, the right panel present how the response should be if f_{stop} command is active, showing that the output power is kept constant until the frequency falls below f_{stop}.

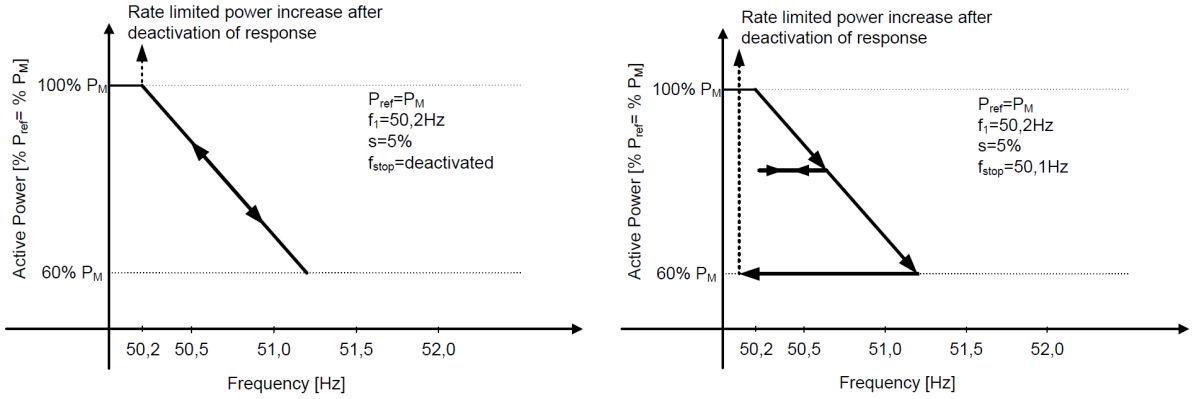

Figure 6: Active power frequency response to over-frequency. Source: [3].

In case of under-frequency, the same approach as in Eq. 3 is used. In Fig. 7 an example of the inverter response to grid under-frequency is shown. For this case it is observed that the f_{stop} command is always deactivated, so the active power frequency response is only deactivated if the frequency increases above $f1$.

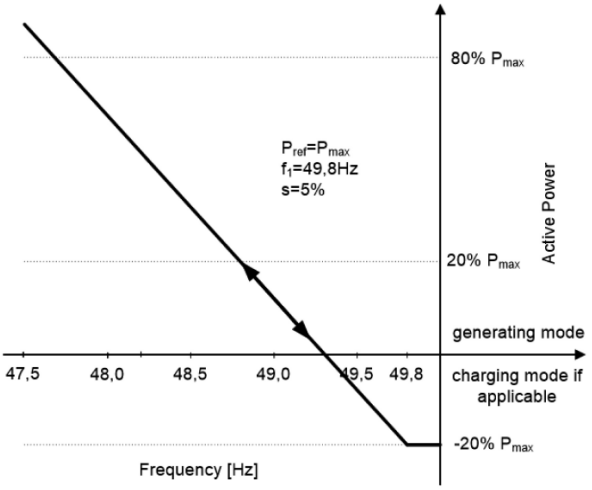

Figure 7: Active power frequency response to under-frequency. Source: [3].

2.5.2 Voltage support by reactive power

The prEN50549-10 defines in its section 5.5.2.4 test procedures to evaluate the response of voltage related control mode for reactive power. It is established that generating plants shall not lead to voltage changes out of acceptable limits, and in case of over-voltage or under-voltage, shall be capable to respond to changes in voltage magnitude. As shown in Fig. 8 the inverter shall be capable to inject/absorb reactive power when the grid voltage is outside the dead band ($V < V_2$ or $V > V_3$), and the injection/absorption is kept constant until lower/upper voltage limit for the inverter is reached. The curve points may vary according to each network code, and the PV inverters are required to perform a proper operation of the voltage control for different configurations.

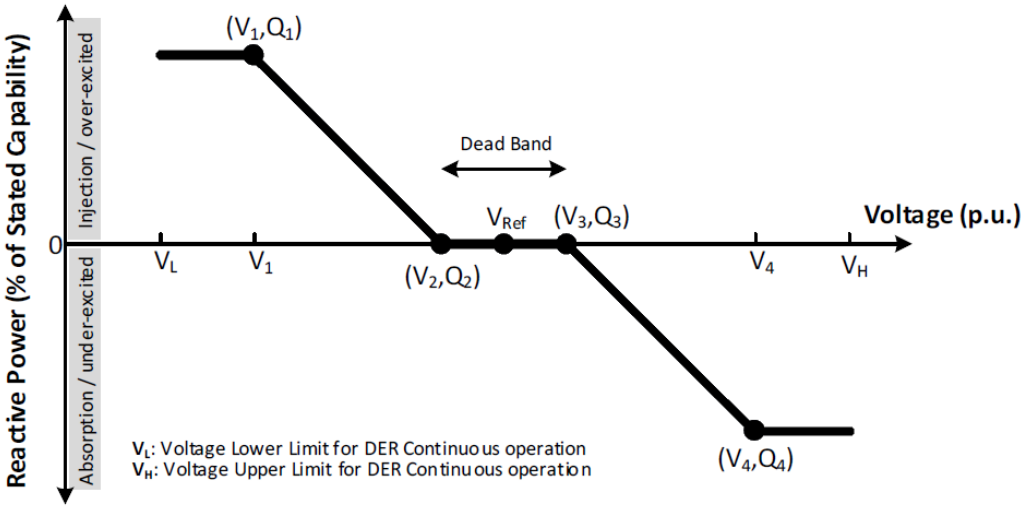

Figure 8: Voltage support by reactive power. Source: [3].

2.5.3 Voltage related active power reduction

The prEN50549-10 defines in the section 5.6 test procedures related to the optional operational capability of active power reduction in case of over-voltage. As shown in Fig. 9 the inverter shall be capable to reduce output power when there is a situation of grid over-voltage ($V > V_2$) and the reduction is kept constant until reaching the voltage upper limit for continuous operation of the inverter (V_2). The value of P_2 is set by the PV inverter manufacturer, and is considered to be the minimum active power value at which the inverter can maintain continuous operation.

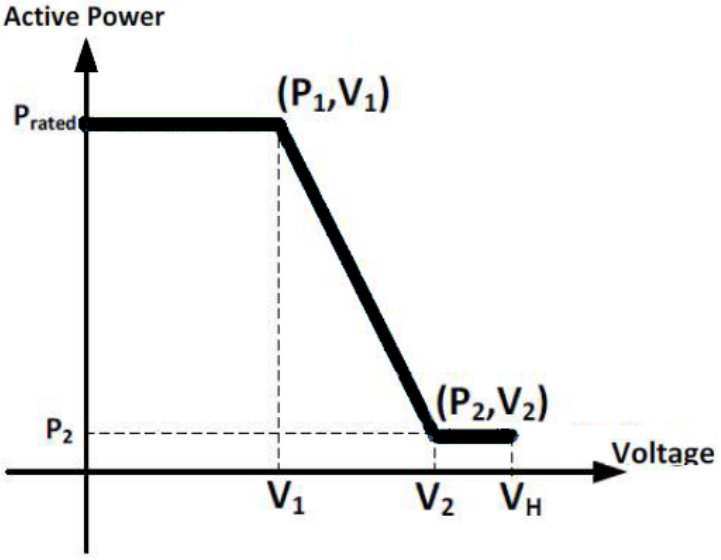

Figure 9: Voltage related active power reduction. Source: [3].

2.6 Hardware In a Loop

To execute the automated grid support function testing of the PV invertes, Hardware in the loop (HIL) is used. HIL is a real-time simulation for embedded control systems, in presence of hardware and other control systems in which a dynamic simulator is replaced by the real system, in that way, in an ideal HIL, the system is substituted with its simulator and other hardware and software are exactly implemented [17]. Fig. 10 shows a simple control loop for an ideal HIL. Implementation of HIL allows to perform the testing and evaluation of the system in real-time, ensuring that the embedded control system can deliver the control input within the desired sampled period [18]. The main difference of HIL with traditional digital real-time simulation is that the last one requires the entire system to be modeled inside the simulator and does not involve external interfacing or Input/Output terminals (I/Os), and in the HIL simulation parts of the fully-digital real-time simulation have been replaced with actual physical components [19].

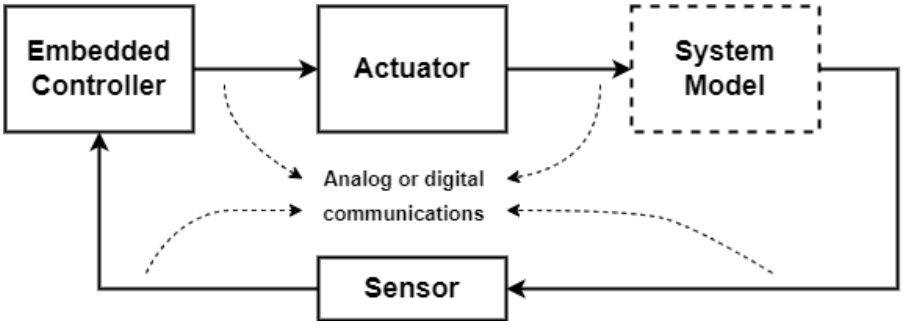

Figure 10: Closed loop control system block diagram for an ideal HIL. Adapted from [17].

If the HIL system involves real controller hardware that interacts with the rest of the simulated system (as is the system used in this study), it is called Controller Hardware-In-the-Loop (CHIL). Using CHIL, no real power transfer takes place, the power system is modeled as a virtual system inside the simulator, and the external controller hardware exchanges controller inputs/outputs with the system inside the simulator [19]. Fig. 11 shows an example of a conceptual CHIL model and the model used for this study. The HIL system used corresponds to a 34.5 kW AIT smart grid converter (SGC) controller connected to a Typhoon HIL 402, thereby constituting the CHIL system.

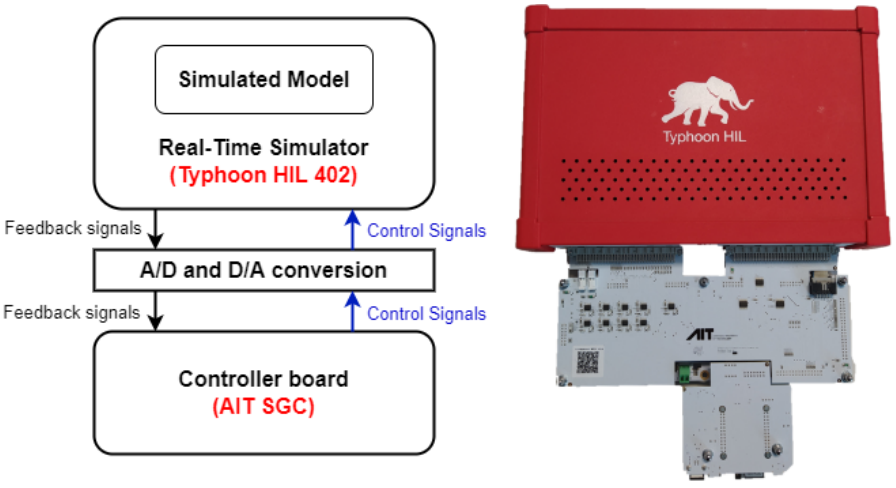

Figure 11: Conceptual model and real model of CHIL. Adapted from [19].

2.7 SunSpec System Validation platform

SunSpec is a global alliance of DER industry participants, to enable "Plug & Play" system interoperability, grid interconnection, and secure data communications for DER technologies. Among its products the SunSpec System Validation Platform (SVP) provides a framework for testing and validating SunSpec compliant devices and applications. Three principal types of testing have been targeted: SunSpec protocol

conformance testing, equipment functional testing, and SunSpec Application Program Interface testing [20]. For this study, SVP is used to autonomously perform the interconnection and interoperability of the certification grid support functions as stated in the prEN50549-10. As shown in Fig. 12, SVP allows communication with the DUT, grid simulator, PV simulator, and data acquisition system.

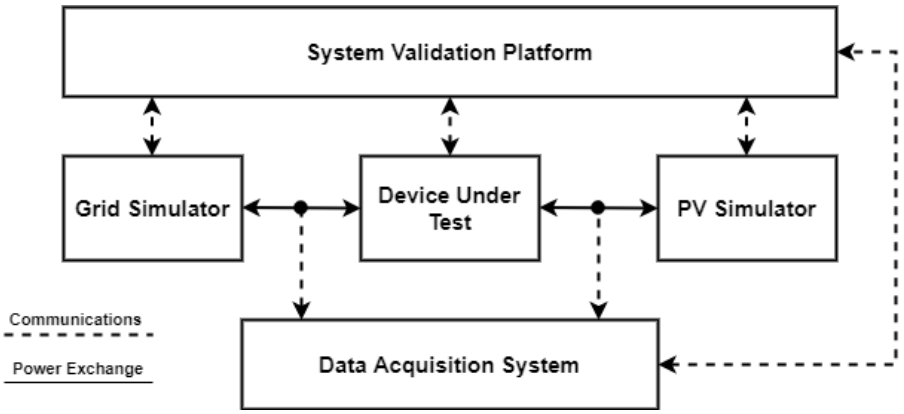

Figure 12: SunSpec System Validation Platform Scheme. Adapted from [2].

SVP has an interface that allows the user to select parameters, define tests, and configure all equipment based on the DUT. As shown in Fig. 13, SVP communicates with the HIL simulator via a USB connection using the Typhoon HIL API, which allows to perform the grid and PV power settings, and data acquisition, and also communicates via SunSpec Modbus TCP over Ethernet, which allows interaction with EUT settings. SVP uses abstraction layers to allow using the same Python Scripts, which means that the same script logic and commands can be used in different test facilities.

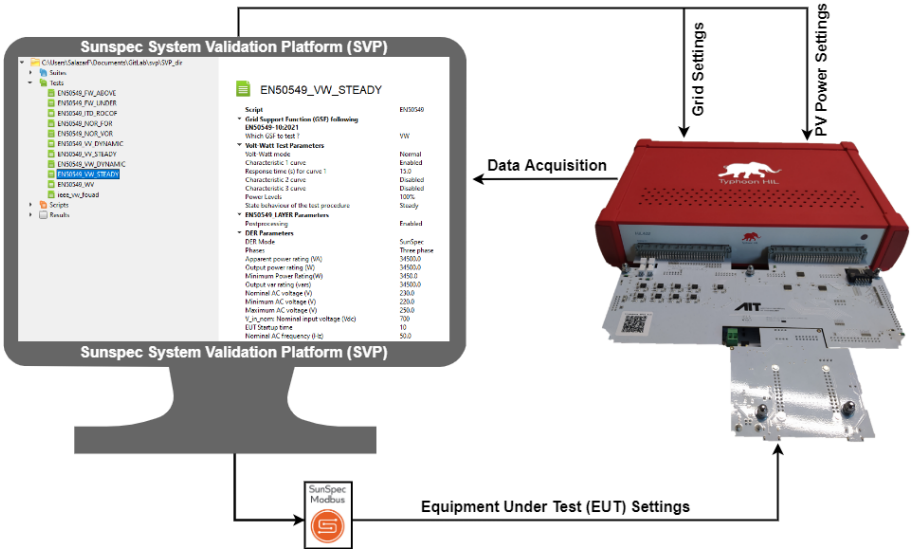

Figure 13: SVP communications with CHIL test configuration.

3 Methodology

Test were conducted with the SVP to assess the grid-support functions of PV inverters following the prEN50549-10 standard. The testbed consists on a real-time simulation system Typhoon HIL 402 and a 34.5 kW three-phase AIT Smart Grid Converter (SGC) controller.

3.1 Simulated model

A general overview of the simulated model is shown in Fig. 14, which illustrates the three main elements of the system: a PV simulator, a grid simulator, and the AIT SGC. For technical information about the AIT SGC and the Typhoon HIL 402, refer to annexes.

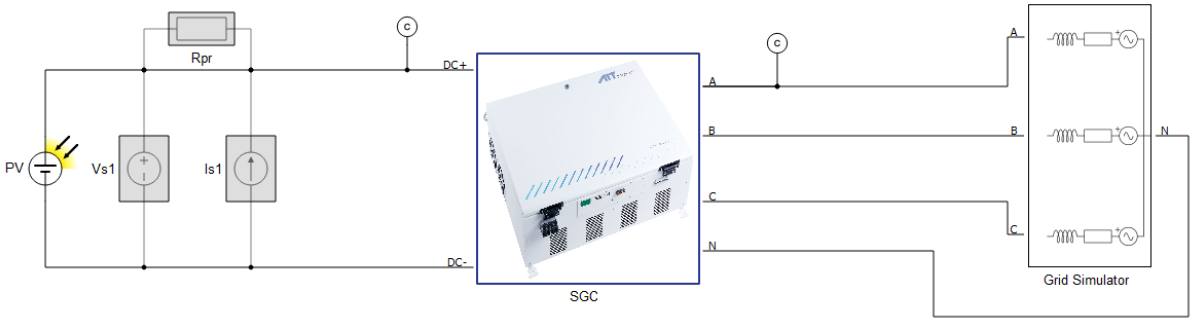

Figure 14: General Schematic Model for the system of the study.

Once the model is compiled, control and monitoring actions are performed with the standalone HIL SCADA system, shown in Fig. 15. From this interface, it is possible to evaluate the values of the voltage and frequency at the inverter terminals. Also, it performs the monitoring of the DC measurements, and allows the activation/deactivation of grid support functions, faults and protections settings, and time constants for the active active and reactive power outputs.

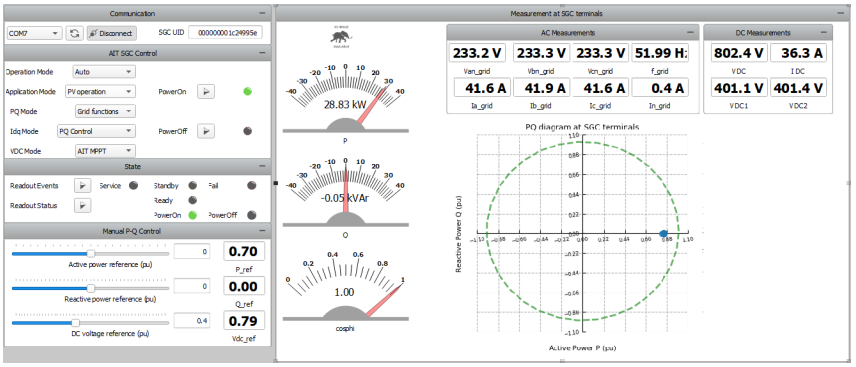

Figure 15: Standalone HIL SCADA system.

3.2 SVP Library Structure

To develop the Python Test Scripts to perform the automation of the processes proposed in the prEN50549-10 standard, a restructuring of the SVP repository previously created for the automation procedures following the IEEE1547.1 according to the studies [2],[4] and [5], was proposed. Fig. 16 shows the general scheme of the new proposed structure, which aims to facilitate the introduction of new standards to the SVP. Once the new structure was established, prEN50549-10 standard test procedures were introduced.

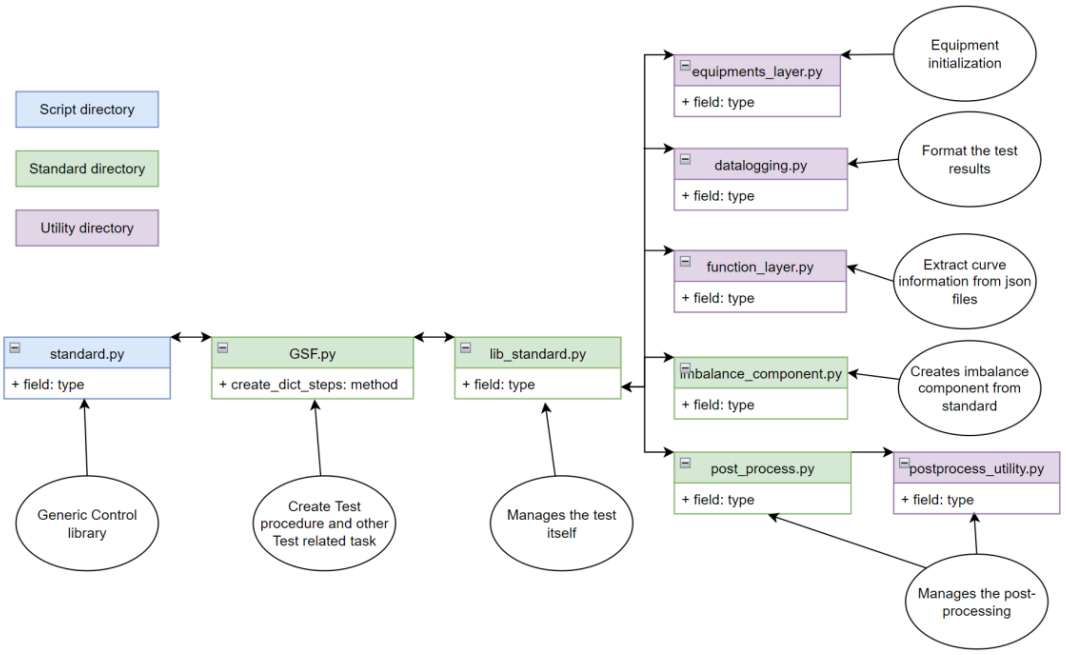

Figure 16: SVP Library restructure for a Generic Standard.

In this way, and following the proposed new SVP structure, an Open-Source repository was created with the Python Test Scripts to execute the procedure for the grid support functions proposed in the prEN50549-10 standard. The following are the hyperlinks to the different segments of the repository:

- SVP General Repository: is a repository that contains all of the Open-Source OpenSVP components written in Python 3.7.
- Standard Library: is a library where all the libraries for each standard are placed. Also contains scripts for the test initialization, connection with equipment, data logging, criteria evaluation, and utility for drivers connection.
- prEN50549-10 Library: is a library that contain all the Python Scripts necessary to perform the test following the prEN50549-10 standard. Within this library are 3

main components:

- EN50549.py: is a generic control script where all the other components are performed using the inheritance method that allows to define a Python class that inherits all the methods and properties from another Python classes.
- EN50549_layer.py: this script manage the test itself and execute procedure as required. Also evaluates the postprocess if the user requests it.
- GridSupportFunction: is a library that contains all the grid support function stated in the prEN50549-10, and create test procedure and other test-related tasks. The following are the grid support function test scripts of interest for this study that are included inside this library: freq_watt_layer.py, volt_var_layer.py, and volt_watt_layer.py

The following are the logical procedures and different configurations that involve each grid support function according to the prEN50549-10 standard, with the proposed Python Test Scripts to perform the automation of each:

3.3 Test procedure: Active response to frequency deviation

The Python Test Script for this procedure correspond to freq_watt_layer.py. The test is carried out for a specific frequency threshold and droop settings established according to the test conditions. For over-frequency, the test settings correspond what is proposed in Table 1, and for under-frequency, the test settings correspond to what is proposed in Table 2.

Table 1: Power response to over-frequencies: Frequency threshold and droop settings.

Curve Setting	**Setting (a)**	**Setting (b)**	**Setting (c)**
Frequency Threshold f_{th} [Hz]	50,2	50,5	50,2
Active Power Droop [%]	5	2	12
Power level at start of test [% P_n]	100 / 50	60	40
Intentional delay [s]	0	0	2
Configured deactivation threshold f_{stop} [Hz]	N.A.	50,5	50,05

Table 2: Power response to under-frequencies: Frequency threshold and droop settings.

Curve Setting	**Setting (a)**	**Setting (b)**	**Setting (c)**
Frequency Threshold f_{th} [Hz]	49,8	49,5	49,8
Active Power Droop [%]	5	2	12
Power level at start of test [% P_n]	0	0	50
Intentional delay [s]	0	0	2
Configured deactivation threshold f_{stop} [Hz]	No	No	No
Active Power Reference P_{ref}	P_{max}	P_{max}	P_{max}

The test must be executed gradually increasing/decreasing the frequency according to the steps proposed in the prEN50549-10 standard section 5.4.3.2 for over-frequency and section 5.4.3.3 for under-frequency, and measuring the power value respectively. In addition, the following is considered:

- The active power target value is calculated for each frequency point according to the configured droop setting and P_{ref} setting.
- The step response behaviour is measured starting from the instant the frequency reaches the end value of the considered frequency point.
- For the step response time and the settling time a tolerance band of ±10% the active power target value is considered.
- The power value is measured considering the mean value over 1 minute.
- The measurement starts from the instant the generated power reaches the active power target value ± 10% of active power for the first time.

3.4 Test procedure: Voltage support by reactive power

The Python Test Script for this procedure correspond to volt_var_layer.py. The test is performed with settings (a) and (b) defined in Table 3. It is important that for three-phase generating unit, as is the case of this study, the voltages shall be applied in a balanced way on all phases. The test is performed to evaluate both steady and dynamic response behaviour of the inverter when changing the output values of the reactive power.

Table 3: Settings for voltage related control mode for reactive power.

Parameter of characteristic	Setting (a)	Setting (b)
Dead band (horizontal section of the characteristic curve around Un) db_{char}	As wide as possible but extending not more than from -6 % Un to +6% Un.	0
Minimum and maximum reactive power of the characteristic Q_{max}	95% of $Q_{max-over}$ and $Q_{max-under}$ respectively	10% of $Q_{max-over}$ and $Q_{max-under}$ respectively
Slope of the steepest section of the characteristic curve	As steep as configurable	As flat as configurable
Time constant	As fast as possible but not slower as 3 s	As slow as possible but not slower as 20 s
Min cos	0,4	Deactivated
Lock-in power	Deactivated	20% Pna
Lock-out power	Deactivated	5 Pnb

To evaluate the steady state the test must be executed gradually increasing/decreasing the grid voltage according to the steps proposed in the prEN50549-10 standard section 5.5.2.4.2, and measuring the reactive power output. To evaluate the dynamic state the test must be executed gradually increasing/decreasing the grid voltage, and at the same time varying the output power according to the steps proposed in the prEN50549-10 standard section 5.5.2.4.3, and recording the output reactive power. In addition, the following is considered:

- The voltage, current, active power and reactive power shall be recorded as 10-period RMS values (positive sequence components for 3-phase generating units).
- The step response behaviour is measured starting from the instance of the voltage jump, and a tolerance band of ± 5% of nominal power to the reactive power set point is considered.
- The static reactive power value is measured considering the mean value over 30 seconds.

3.5 Test procedure: Voltage related active power reduction

The Python Test Script for this procedure correspond to volt_watt_layer.py. No specific setting conditions of the curve are established in prEN50549-10 standard for this test, however, it is performed with settings defined in Table 4. It is important that for three-phase generating unit, as is the case of this study, the voltages shall be applied in a balanced way on all phases. The test is performed to evaluate both steady and dynamic response behaviour of the inverter when changing the output values of the active power.

Table 4: Settings for voltage related to active power reduction.

Curve settings	
V_1	106% Un
P_1	P_{rated}
V_2	110% Un
P_2	20 % P_{rated} or P_{rated}

The test must be executed with the same considerations as for the test procedure related to voltage support by reactive, with the difference that for this test the grid voltage must be gradually increased/decreased according to the steps proposed in the prEN50549-10 standard section 5.6.3 for steady state and section 5.6.4 for dynamic state, and measuring the active power value respectively.

4 Results

Once all the necessary Python Tests Scripts have been developed to carry out the automation of the grid support function proposed in the prEN50549-10 standard, results are obtained through the data acquisition system of Typhoon HIL using the Typhoon HIL Python API every 200 ms from analog signals representing the AC and DC current and voltage, and from calculated CHIL channels it is obtained the root mean square (RMS) and positive sequence values for AC power, reactive power, and power factor. It is important to note that for some tests it is necessary to perform the procedure with different irradiance levels, However, only the overall results of each of the tests are presented to demonstrate automation accuracy. For test results at different irradiance levels, please refer to the annexes section.

4.1 Test results: Active response to frequency deviation

The tests were performed as described in Section 3.3. The result for the over-frequency setting (a) is presented in Fig. 17, showing the inverter's active power behavior with increasing grid frequency. The maximum frequency was set to 52 Hz as stated in the standard, and the test is performed by regulating the frequency of the grid simulator in order to reproduce the different frequency conditions until the maximum value is reached and then return to the nominal value.

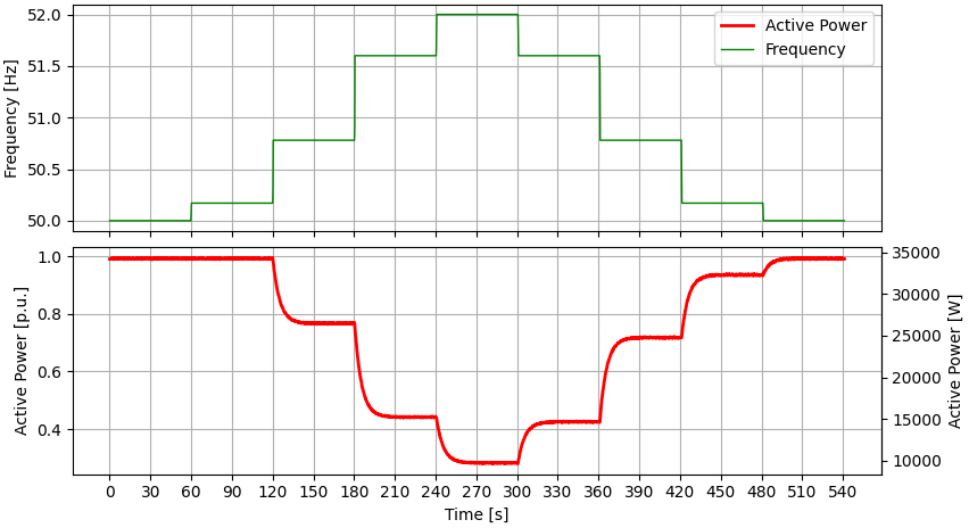

Figure 17: Test result: Power response to over-frequencies - Setting (a).

The results for over-frequency settings (b) and (c) are illustrated in Fig. 18. Note that for both tests the active power initial output is lower than the nominal value, as stated in

the Table 1. In addition, it is observed that once the grid frequency begins to return to its nominal values, the inverter does not inject all the nominal power allowed until it has passed the configured deactivation threshold as the command for f_{stop} is active for these settings.

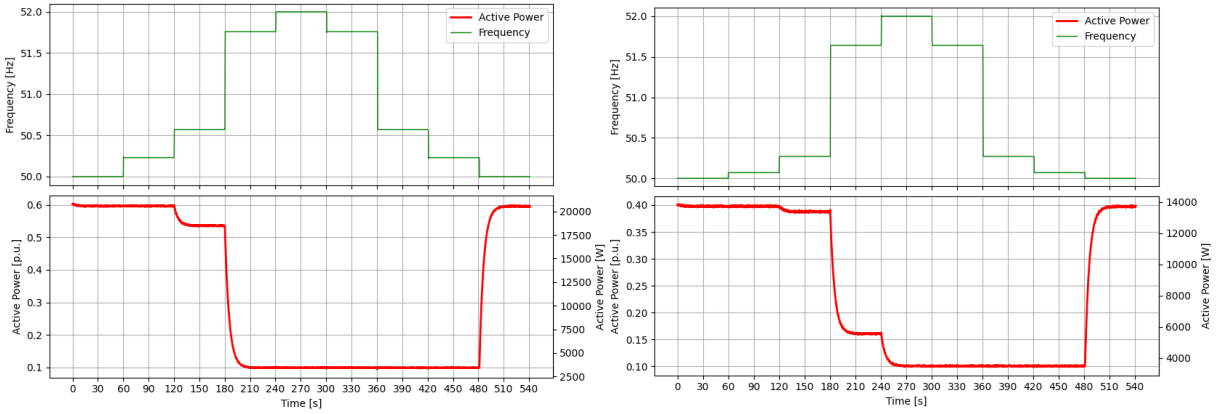

Figure 18: Test result: Power response to over-frequencies - Setting (b) and (c).

For under-frequency, the results obtained for setting (a) are illustrated in Fig. 19, showing the inverter's active power behavior with decreasing grid frequency. For this case, 47 Hz was set as the minimum frequency as stated in the standard, and the active power initial output is considered to be zero as the charging mode of the inverter is not considered for this study.

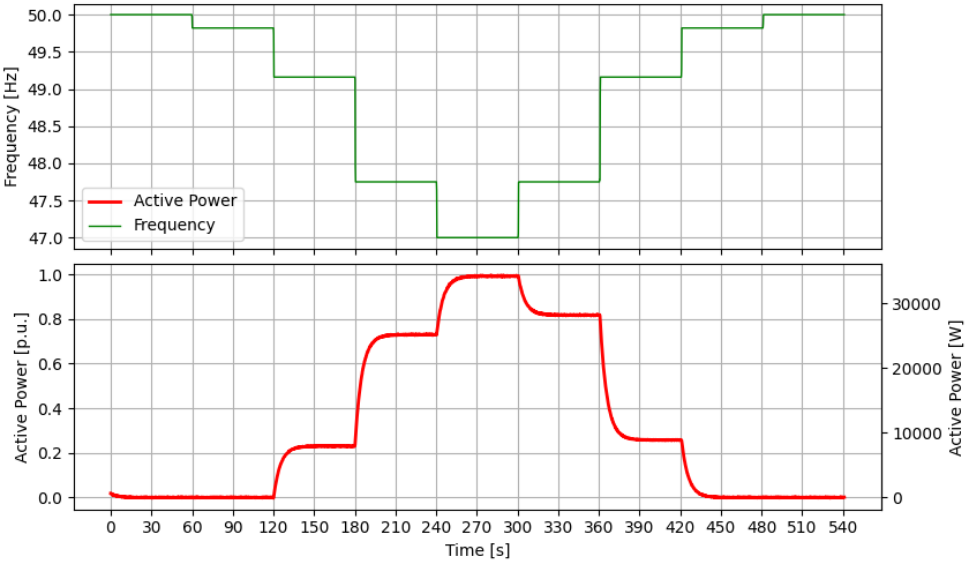

Figure 19: Test result: Power response to under-frequencies - Setting (a).

The results for under-frequency settings (b) and (c) are illustrated in Fig. 20, showing that for both tests the active power injected by the inverter starts from zero or from the

established percentage of the nominal active power as indicated in Table 2, and once the lowest frequency point is reached, the inverter starts injecting active power into the grid to try to increase the grid frequency.

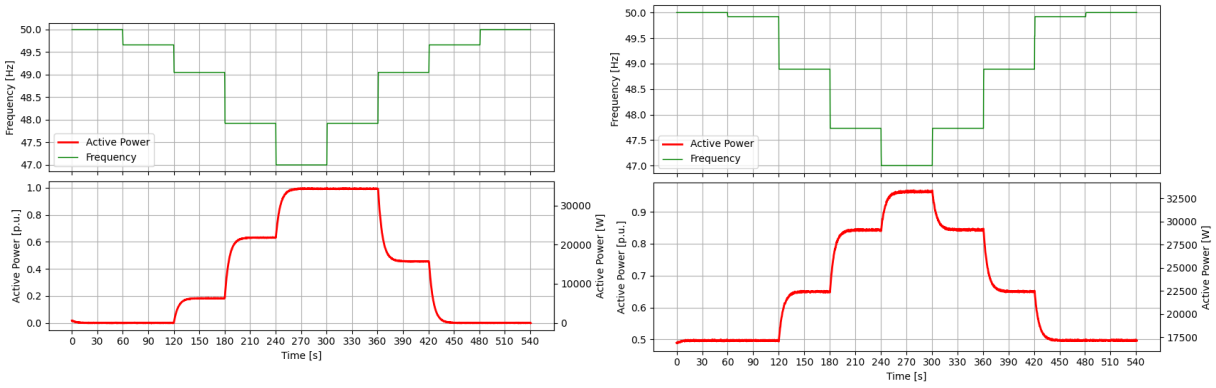

Figure 20: Test result: Power response to under-frequencies - Setting (b) and (c).

4.2 Test results: Voltage support by reactive power

The tests are performed as described in Section 3.4. For this test, two procedures are carried out in order to evaluate the steady and dynamic behavior. The results for the steady behaviour obtained for the setting (a) stated in the Table 3, are shown in the Fig. 21. Note that when there is an under-voltage situation, and the grid voltage value is below the dead band, the inverter injects reactive power, and when an over-voltage situation occurs, and the grid voltage value is above the dead band, the inverter absorbs reactive power.

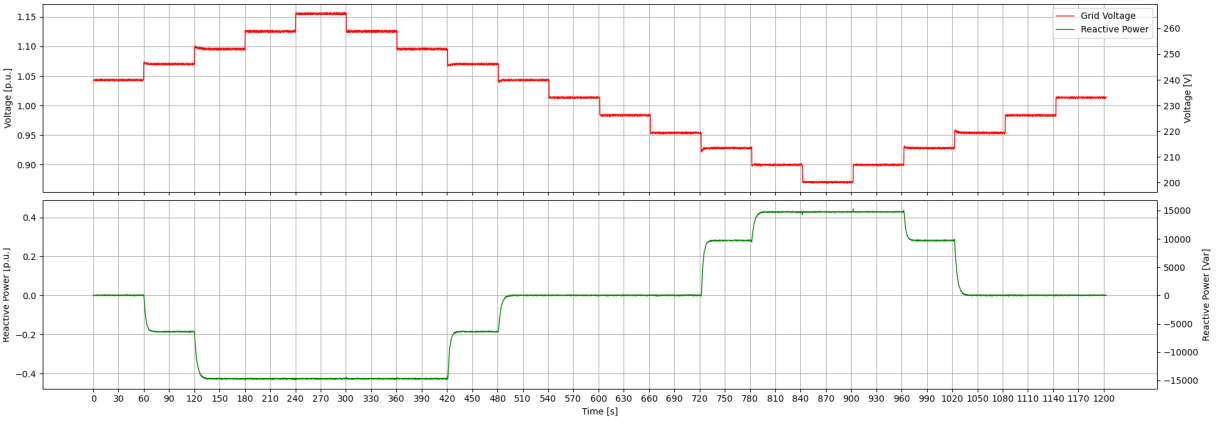

Figure 21: Test result: Voltage related control mode for reactive power (Steady state behaviour) - Setting (a).

The result for steady behaviour setting (b) is illustrated in Fig. 22, and shows that in the absence of a dead band, when the grid voltage varies below or above the nominal

value, the inverter immediately injects or supplies reactive power, accordingly. It is also shown that unlike the test for configuration (a), for configuration (b) it is only allowed to inject/absorb up to 10% of the allowed rated reactive power value.

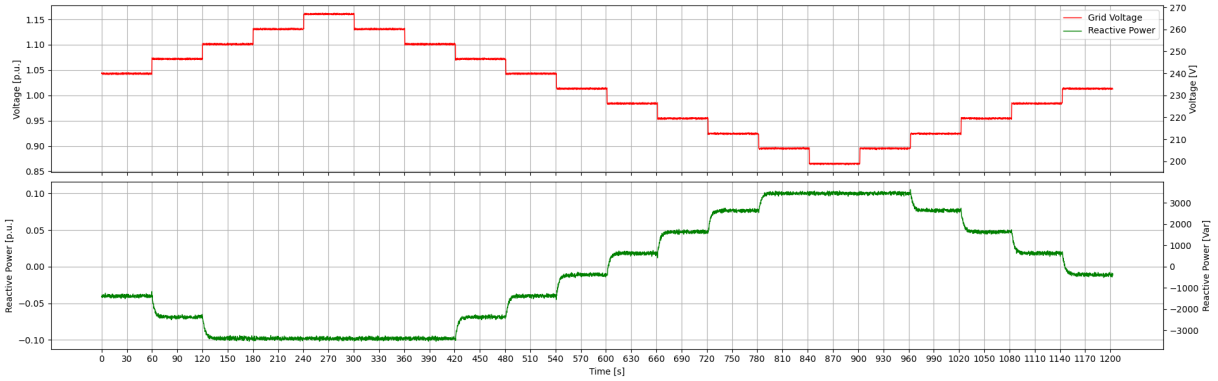

Figure 22: Test result: Voltage related control mode for reactive power (Steady state behaviour) - Setting (b).

The results obtained for test procedure for dynamic state behaviour according to setting (a) stated in the Table 3, are shown in Fig. 23. Note that when the grid voltage varies, the reactive power control is immediately activated. Also, when the inverter's active power output varies, the reactive power control remains totally dependent on the voltage values. It is also important to verify that when the active power values are at their lowest point, and the reactive power values are at their highest, the inverter does not trip, thereby meeting the minimum requirements required for this test.

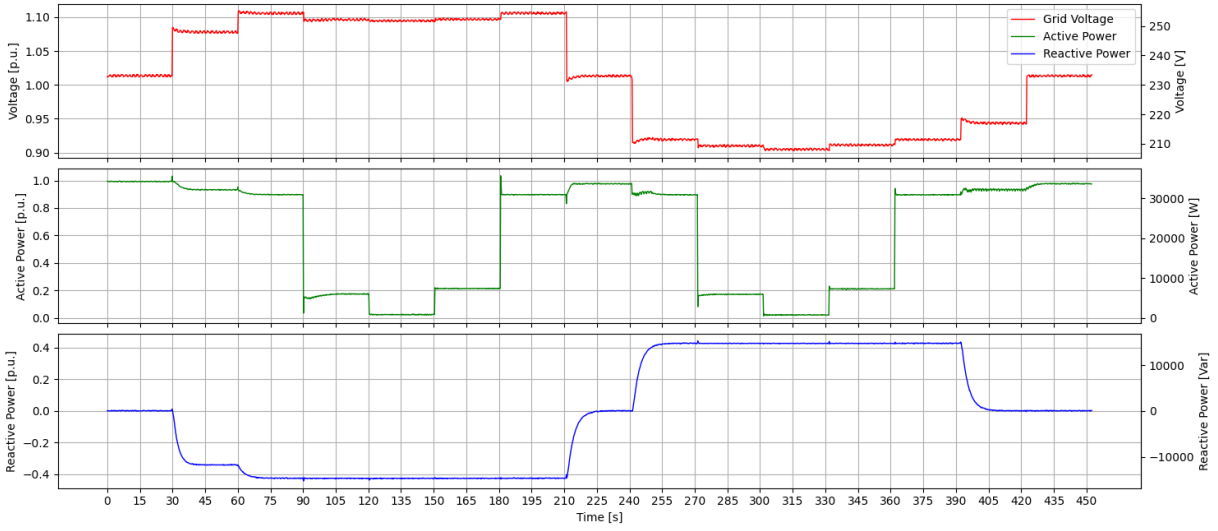

Figure 23: Test result: Voltage related control mode for reactive power (Dynamic state behaviour) - Setting (a).

The result for dynamic behaviour setting (b) is illustrated in Fig. 24. In this case, since the percentage of reactive power is lower (10%), when varying the active power, small peaks are observed, However, these are within the 10% variation allowed.

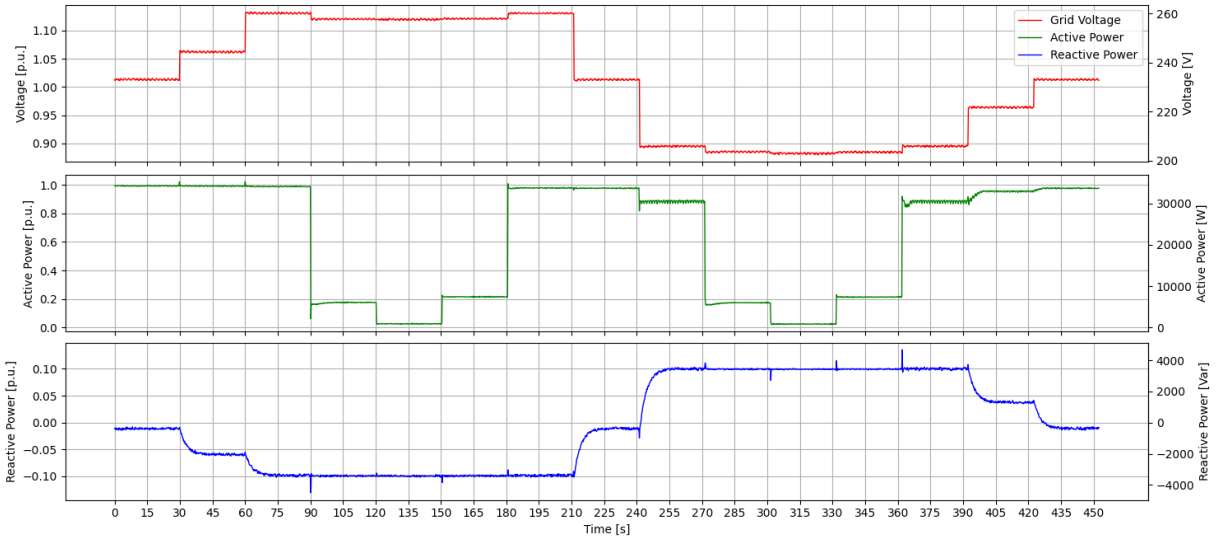

Figure 24: Test Result: Voltage related control mode for reactive power (Dynamic state behaviour) - setting (b).

For both settings the influence of the output active and reactive power on the grid voltage was verified. As indicated in the Eq. 1, it is expected that as the injection of active power by the inverter decreases, the value of the grid voltage is affected by decreasing its rating. This is noticeable in the two tests results when the active power decreases from its nominal value and the grid voltage consequently presents a slight decrease. It is also appreciated that the as the PV inverter begins the absorption of reactive power, that leads to to a gradual decrease of the grid voltage, and when the injection of reactive power occurs, the grid voltage suffers a gradual increase instead.

4.3 Test results: Voltage related active power reduction

The tests are performed as described in Section 3.5. For this test, two procedures are carried out in order to evaluate the steady and dynamic behavior. The result for the steady behaviour is shown in Fig. 25 and is verified that the inverter output active power decreases when there is an over-voltage situation in the grid, and then returns to its maximum value when the grid voltage recovers its nominal value. For this particular case, it is interesting to evaluate the influence of the active power on the grid voltage. After 180 seconds, it is observed that the control of the grid voltage starts when the active power decreases, and it is noticeable how slightly decreases the grid voltage.

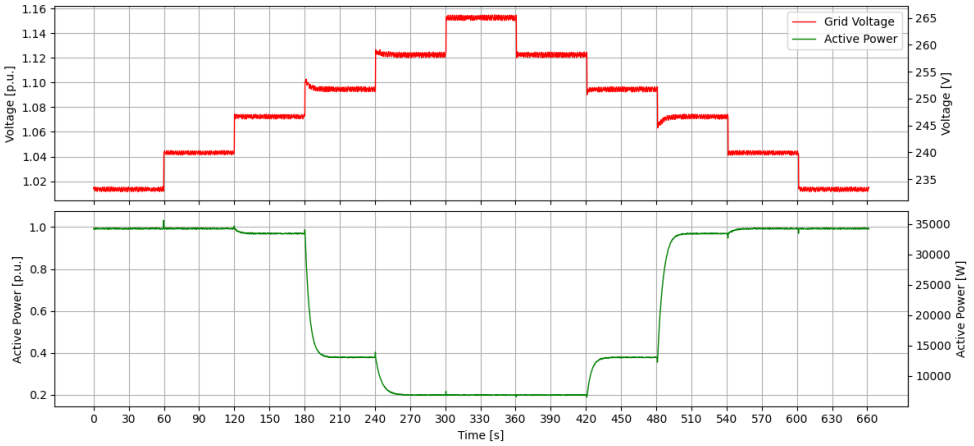

Figure 25: Test Result: Voltage related to active power reduction - Steady state behaviour.

To observe in more detail how the variation of the active power influences the grid voltage, the result obtained for test procedure for dynamic state behaviour is presented in Fig. 26.

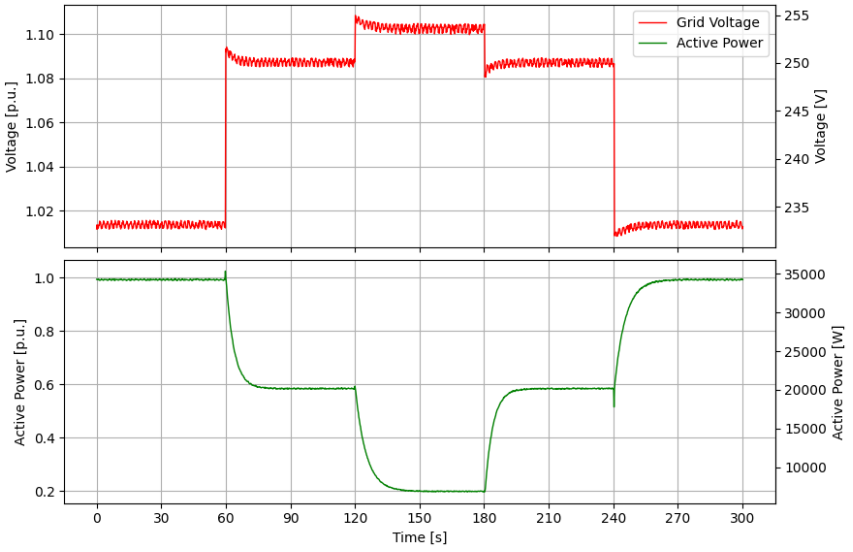

Figure 26: Test Result: Voltage related to active power reduction - Dynamic state behaviour.

The results for the dynamic state test are similar to those observed for the steady. In this case, when the grid voltage value increases outside the normal operating values, the PV inverter is forced to reduce the active power output, and it can be observed that this action has a slight influence on the grid voltage, which is slightly reduced. When the grid voltage values return to their nominal values, it is observed that the opposite happens, the PV inverter output active power increases and this slightly increases the grid voltage.

5 Discussion

The automation of the procedure required for each test was carried out, as well as the automation of the corresponding processes to evaluate whether a test complies with the minimum requirements of the EN50549-10 standard. This section focuses on the post-process Python scripts where it is determined if a test was passed. The Post-Process Library inside the prEN50549-10 Library includes three main scripts for the evaluation of the tests:

- EN50549_postprocess.py: is a general post-process script where the evaluation for all the test is performed.
- gsp_curves.py: is a script that performs the plotting for the results related to the whole process for all the grid support functions.
- low_pass_filter.py: some result test related to the grid support functions needs to be evaluated and compared with a low pass filter. Therefore, this script takes the target and measured values of each test and performs the respective comparison.

The assessments criteria established for each grid support function according to the prEN50549-10 standard is evaluated for the results showed in Section 4 of this study. In addition, some plots are presented to evaluate the response for some specific steps as required for each procedure.

5.1 Assessment criteria: Active response to frequency deviation

For the results obtained, as well as for the over-frequency and under-frequency tests, section 5.4.4 of the prEN50549-10 establishes that the tests are passed if:

- For each frequency point, the deviation between the expected and the measured value of active power falls within the required tolerance: $\pm$ 10 % of the nominal active power, evaluated with a 1 minute average value.
- The step response time is less than the required value, for this case 30 seconds.

Once the above is known, the results obtained in the Section 4.1 of this study are evaluated according to the respective criteria. Table 5 and Table 6 show the evaluation criteria for the over-frequency and under-frequency test setting (a), respectively. Note that the admissible range of each active power value and the actual value measured for each test step is shown, and in both evaluations, for all steps, all criteria required by the standard are fulfilled.

Table 5: Criteria Validation: Active response to frequency deviation - Power response to Over-frequencies.

Step	**Measured Frequency [Hz]**	**Measured Active Power [p.u.]**	**Criteria P_{min} [p.u.]**	**Criteria P [p.u.]**	**Criteria P_{max} [p.u.]**	**Criteria Active Power**
Step A	50	0.99	0.9	1	1.1	Pass
Step B	50.17	0.99	0.9	1	1.1	Pass
Step C	50.78	0.79	0.67	0.77	0.87	Pass
Step D	51.59	0.47	0.34	0.44	0.54	Pass
Step E	52	0.3	0.18	0.28	0.38	Pass
Step F	51.61	0.41	0.34	0.44	0.54	Pass
Step G	50.8	0.69	0.66	0.76	0.86	Pass
Step H	50.18	0.91	0.9	1	1.1	Pass
Step I	50	0.99	0.9	1	1.1	Pass

Table 6: Criteria Validation: Active response to frequency deviation - Power response to Under-frequencies.

Step	**Measured Frequency [Hz]**	**Measured Active Power [p.u.]**	**Criteria P_{min} [p.u.]**	**Criteria P [p.u.]**	**Criteria P_{max} [p.u.]**	**Criteria Active Power**
Step A	50	0	-0.1	0	0.1	Pass
Step B	49.82	0	-0.1	0	0.1	Pass
Step C	49.16	0.21	0.15	0.25	0.35	Pass
Step D	47.76	0.72	0.72	0.82	0.92	Pass
Step E	47.01	0.97	0.9	1	1.1	Pass
Step F	47.74	0.83	0.72	0.82	0.92	Pass
Step G	49.14	0.31	0.17	0.27	0.37	Pass
Step H	49.81	0.03	-0.1	0	0.1	Pass
Step I	50	0	-0.1	0	0.1	Pass

To evaluate graphically whether the active power response of each step is within the permitted tolerance band, Fig. 27, which represent the evaluation of the active power response for the step C in the test of over-frequency, is presented as an example. Note that the user may request for this optional evaluation in the SVP interface. For this case, it is observed that when the frequency increases above the frequency threshold established for setting (a) in Table 1 (50.2 Hz for this case), the active power supplied by the inverter decreases until reaching the requested target. It is considered that it must be less than 10 seconds since active power measurement (green curve) enters the tolerance band, which is perfectly fulfilled for this step and this particular test.

Finally, by verifying that all the procedures and the subsequent evaluation of the results obtained for the active response to frequency deviation tests have been executed correctly, it is established that the automation for this test has been performed successfully.

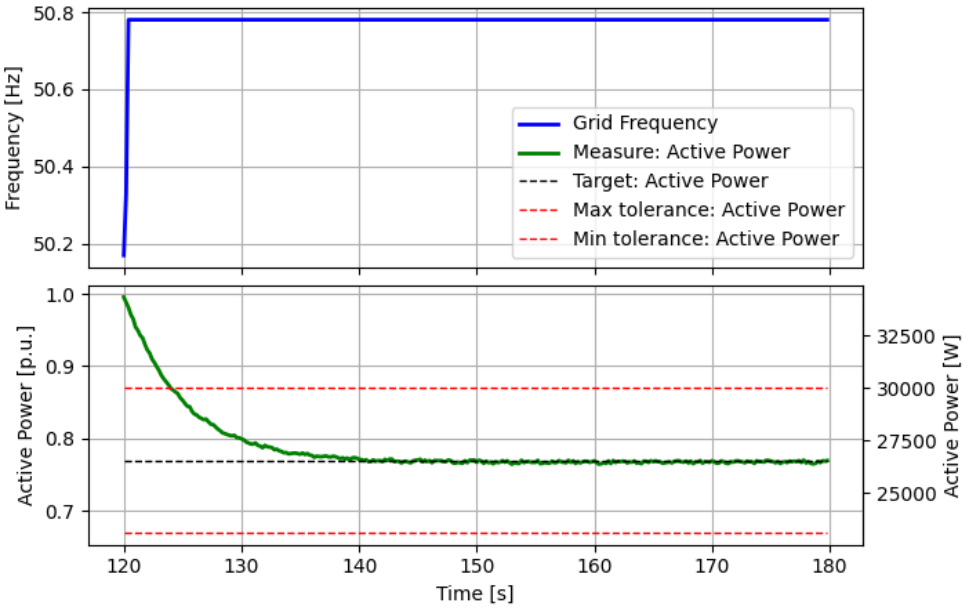

Figure 27: Evaluation of active power reduction for over-frequency.

5.2 Assessment criteria: Voltage related control mode for reactive power

For the results obtained for these tests, section 5.5.2.4.4 of the prEN50549-10 establishes that the tests are passed if:

- The measured 30-seconds averages of the reactive power (positive sequence components) during steady state conditions are within a tolerance band of ±1% nominal voltage.
- The time response of the reactive power during the measurement is within the tolerance band resulting from the behaviour of an equivalent first order filter element and the configured time constant tau (considered as 5 seconds for this study). Accepted tolerances are ±5 % of the nominal power for the reactive power values and 3 seconds for the time delay deviating from an ideal first order filter response.
- No discontinuities in the characteristic curve are detected and no oscillations of the reactive power after the end of the transient period.

The results obtained in Section 4.2 of this study are evaluated according to the respective criteria. As an example, the evaluation of the results obtained for the test corresponding to the steady state setting (a), previously illustrated in Fig. 21, are shown in Table 7. It can be observed that all the steps executed comply with the voltage criteria and active power criteria with the exception of the steps B, H and Q. This can be attributed to the hysteresis involved in the process, as well as the voltage difference

at the inverter terminals which are not taken into account in the evaluation and could slightly affect the target accuracy.

Table 7: Criteria Validation: Voltage related control mode for reactive power (Steady Behaviour) - Setting (a).

Step	Measured Voltage [V]	Measured Voltage [p.u]	Criteria V_{min} [V]	Criteria V_{target} [V]	Criteria V_{max} [V]	Criteria Voltage	Measured Reactive Power [Var]	Measured Reactive Power [p.u]	Criteria Q_{min} [Var]	Criteria Q_{target} [Var]	Criteria Q_{max} [Var]	Criteria Reactive Power
Step A	239.93	1.043	237.50	239.9	245.30	Pass	38.47	0.00	-1725.0	0	1725.00	Pass
Step B	246.13	1.070	244.33	246.8	252.27	Pass	-6390.33	-0.19	-5591.7	-5886	-6180.30	Fail
Step C	252.03	1.096	251.16	253.7	259.24	Pass	-14702.92	-0.43	-14289.9	-15042	-15794.10	Pass
Step D	258.83	1.125	257.99	260.6	266.21	Pass	-14700.09	-0.43	-14289.9	-15042	-15794.10	Pass
Step E	265.69	1.155	264.83	267.5	273.18	Pass	-14693.08	-0.43	-14289.9	-15042	-15794.10	Pass
Step F	258.99	1.126	257.99	260.6	266.21	Pass	-14693.67	-0.43	-14289.9	-15042	-15794.10	Pass
Step G	252.15	1.096	251.16	253.7	259.24	Pass	-14702.45	-0.43	-14289.9	-15042	-15794.10	Pass
Step H	246.28	1.071	244.33	246.8	252.27	Pass	-6610.85	-0.19	-5591.7	-5886	-6180.30	Fail
Step I	240.12	1.044	237.50	239.9	245.30	Pass	-188.78	-0.01	-1725.0	0	1725.00	Pass
Step J	233.39	1.015	230.67	233	238.33	Pass	29.21	0.00	-1725.0	0	1725.00	Pass
Step K	226.58	0.985	223.84	226.1	231.36	Pass	35.33	0.00	-1725.0	0	1725.00	Pass
Step L	219.77	0.956	217.01	219.2	224.39	Pass	38.37	0.00	-1725.0	0	1725.00	Pass
Step M	213.85	0.930	210.18	212.3	217.42	Pass	9127.97	0.26	8387.6	8829	9270.45	Pass
Step N	207.41	0.902	203.35	205.4	210.45	Pass	14415.59	0.42	14289.9	15042	15794.10	Pass
Step O	200.71	0.873	196.52	198.5	203.49	Pass	14764.67	0.43	14289.9	15042	15794.10	Pass
Step P	206.42	0.897	203.35	205.4	210.45	Pass	14770.78	0.43	14289.9	15042	15794.10	Pass
Step Q	212.89	0.926	210.18	212.3	217.42	Pass	10151.07	0.29	8387.6	8829	9270.45	Fail
Step R	218.84	0.951	217.01	219.2	224.39	Pass	937.23	0.03	-1725.0	0	1725.00	Pass
Step S	225.53	0.981	223.84	226.1	231.36	Pass	37.46	0.00	-1725.0	0	1725.00	Pass
Step T	232.39	1.010	230.67	233	238.33	Pass	41.11	0.00	-1725.0	0	1725.00	Pass

To verify graphically that all the steps are within the allowed tolerance band, Fig. 28 is presented. Note that the user may request for this optional evaluation in the SVP interface. For this test, it is observed that all points are within the tolerance band allowed, and the behavior of the corresponding graph of the curve for voltage related control mode for reactive power is followed. It is also observed that all the points are within the allowed tolerance band (including steps B, H and Q), therefore, even though some points do not slightly meet the required tolerance for reactive power, when evaluated together with the voltage criterion, the test is passed.

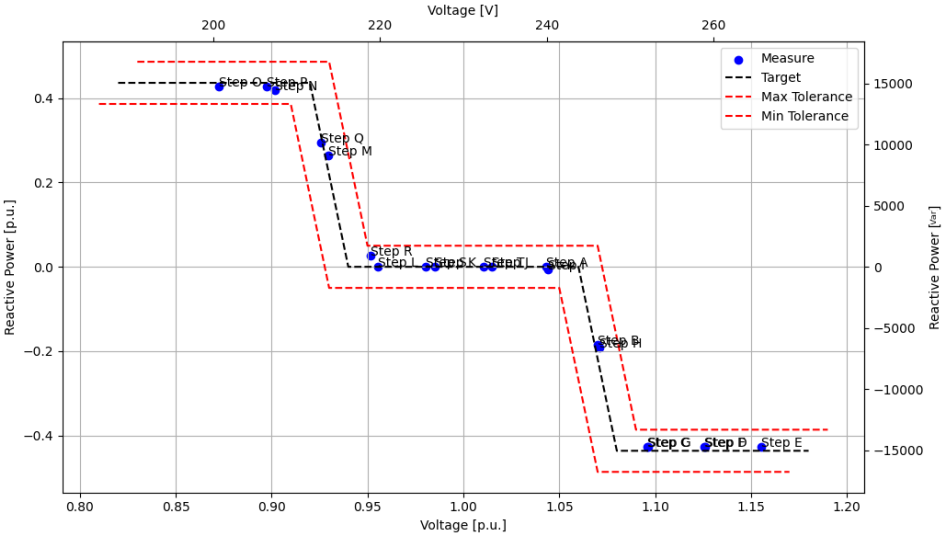

Figure 28: Test result: Voltage related control mode for reactive power - Curve with steps results (steady state) - Setting (a).

To evaluate the tolerance band resulting from the behaviour of an equivalent first order filter element, the user may request for this optional evaluation in the SVP interface for each step. Fig. 29 represents an example for the step response behavior for step C according to the test for Voltage related control mode for reactive power, steady state, setting (a). Note that the set value for this step varies from -5886 Var to -15042 Var, and the measure value adjust to the first order filter response within the tolerance band.

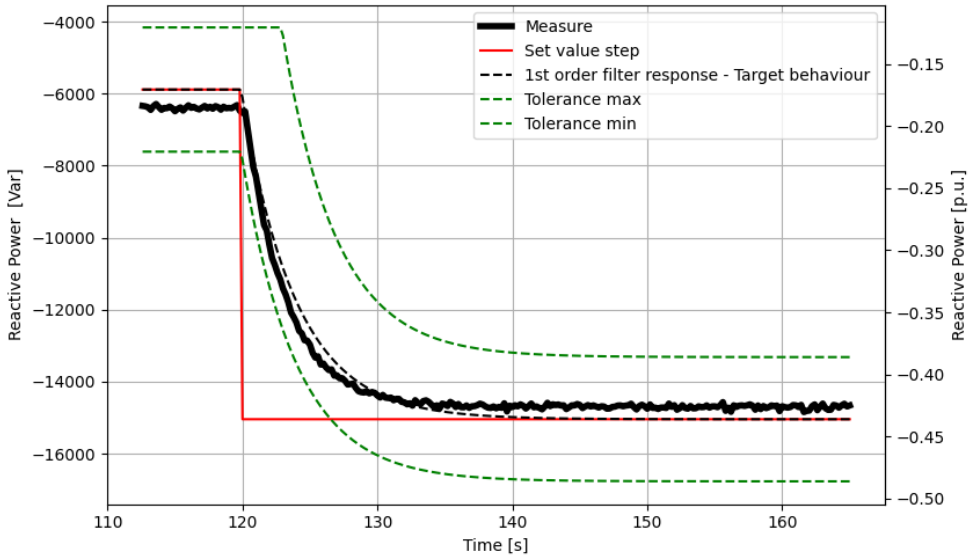

Figure 29: Test result: Voltage related control mode for reactive power (steady state) - Setting (a) - Step response behavior for step C.

Finally, by verifying that all procedures and the subsequent evaluation of the results obtained for the voltage related control mode for reactive power test have been executed correctly, it is established that the automation for this test has been performed successfully.

5.3 Assessment criteria: Voltage related to active power reduction

Section 5.6.5 of the prEN50549-10 establishes that, unless further requirements apply for a specific grid code, the test shall be considered passed if:

- The measured 30-seconds averages of the active power (positive sequence components) during steady state conditions are within a tolerance band of ±1% nominal voltage.
- The time response of the active power during the measurement represents the applied configuration within the tolerance band resulting from the behaviour of an equivalent first order filter element and the configured time constant. The tolerances

are ±5% of nominal power for the active power values and 3 seconds for the time in case of a power decrease/increase.

- No discontinuities in the characteristic curve are detected and no oscillations of the active power after the end of the transient period, and no disconnection of the inverter occur.

The results obtained in the Section 4.3 of this study are evaluated according the respective criteria. As an example, the evaluation of the results obtained for the test corresponding to the steady state, previously illustrated in Fig. 23, are shown in Table 8. It can be observed that all the steps executed comply with the voltage criteria and active power criteria with the exception of the steps E, H and I. This can be attributed to the hysteresis involved in the process, as well as the voltage difference at the inverter terminals which are not taken into account in the evaluation and could slightly affect the target accuracy.

Table 8: Criteria Validation: Voltage related to active power reduction - Test procedure for steady state behaviour.

Step	Measured Voltage [V]	Criteria V_{min} [V]	Criteria V_{target} [V]	Criteria V_{max} [V]	Criteria Voltage	Measured Active Power [W]	Criteria P_{min} [W]	Criteria P_{target} [W]	Criteria P_{max} [W]	Criteria Active Power
Step A	233.82	227.7	230	235.3	Pass	34035.78	32775	34500	36225	Pass
Step B	240.65	234.531	236.9	242.269	Pass	34033.87	32775	34500	36225	Pass
Step C	247.13	241.362	243.8	249.238	Pass	32999.46	32775	34500	36225	Pass
Step D	252.42	248.193	250.7	256.207	Pass	14344.47	13110	13800	14490	Pass
Step E	258.69	255.024	257.6	263.176	Pass	7572.14	6555	6900	7245	Fail
Step F	264.85	261.855	264.5	270.145	Pass	6887.44	6555	6900	7245	Pass
Step G	257.94	255.024	257.6	263.176	Pass	6852.2	6555	6900	7245	Pass
Step H	251.79	248.193	250.7	256.207	Pass	12359.39	13110	13800	14490	Fail
Step I	246.45	241.362	243.8	249.238	Pass	30422.35	32775	34500	36225	Fail
Step J	239.96	234.531	236.9	242.269	Pass	33932.73	32775	34500	36225	Pass
Step K	233.36	227.7	230	235.3	Pass	33997.92	32775	34500	36225	Pass

To verify graphically that all the steps are within the allowed tolerance band, Fig. 30 is presented. Note that the user may request for this optional evaluation in the SVP interface. For this test, it is observed that all points are within the tolerance band allowed, and the behavior of the corresponding graph of the curve for voltage related to active power reduction is followed. Note that all the points are within the allowed tolerance band (including steps E, H and I), therefore, even though some points do not slightly meet the required tolerance for active power, when evaluated together with the voltage criterion, the test is passed.

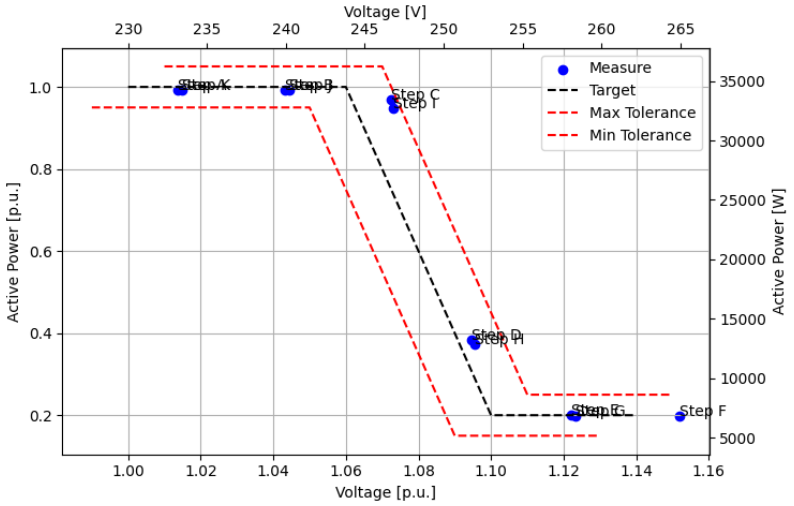

Figure 30: Test result: Voltage related to active power reduction curve with steps results - Setting (a).

To evaluate the tolerance band resulting from the behaviour of an equivalent first order filter element, the user may request for this optional evaluation in the SVP interface for each step. Fig. 31 represents an example for the step response behavior for step D and step I according to the test for voltage related to active power reduction, steady state. Note that the set value for this step varies from 34500 W to 13800 W (left figure) and from 13800 W to 34500 W (right figure), and the measure value adjusts to the first order filter response within the tolerance band.

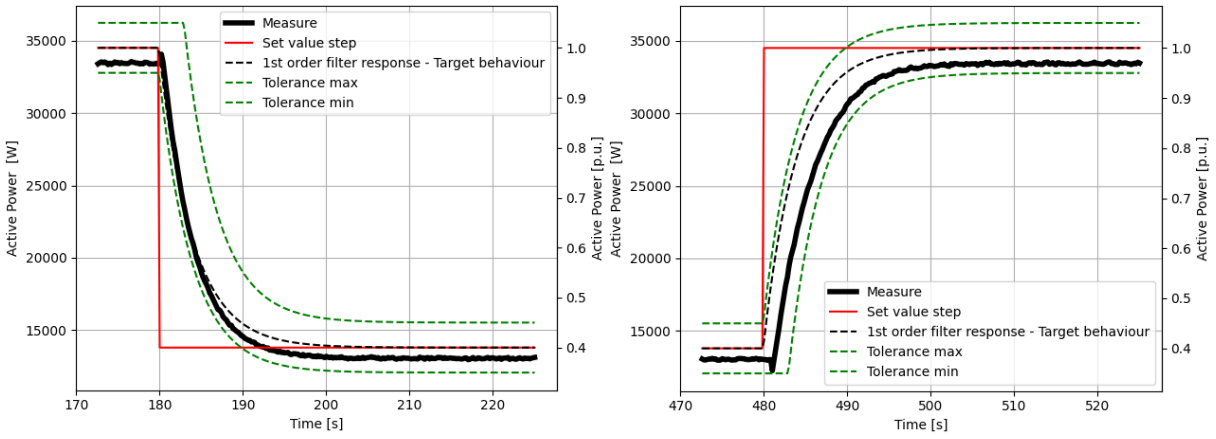

Figure 31: Test result: Voltage related to active power reduction (steady state) - Step response behavior for step D and step I.

Finally, by verifying that the procedures and the evaluation of the results obtained for the voltage related to active power reduction test have been executed correctly, it is established that the automation for this test has been performed successfully.

6 Conclusions

Python Test Scripts to automate certification procedures for grid support functions of the prEN50549-10 standard were successfully developed and evaluated. Achieving the automation of these certification procedures is key to dealing with a high demand for certification of the PV inverters and facing a rapid deployment and integration of smart grid technologies into the grid. The example results obtained the certification procedures of the grid support functions of "Active response to frequency deviation", "Voltage support by reactive power", and "Voltage related to active power reduction" demonstrated the advantages of process automation for tests that typically include hundreds of measurements, which, when carried out manually, would involve a considerable amount of time. Furthermore, the effectiveness of the developed Pythons Test Script was demonstrated by evaluating the results following the assessment criteria of the prEN50549-10 standard, and successfully meeting all the requirements.

To verify the PV inverter controller performance before hardware integration, the use of a CHIL system proved to be highly efficient for the certification process employed, avoiding the use of complex and expensive laboratory equipment, and proving to be a solution to the growing demand for PV converter certification as the use of PV systems increases worldwide. Moreover, as the communication with the CHIL simulator relies on the SVP system by using abstraction layers, the resulting Python Test Scripts can be used for different laboratory testbeds by merely changing the equipment drivers for each testbed. In this way, this methodology can be applied to any power system testing laboratory in the world. Also, it should be noted that this research took a step further and proposed the modification of the traditional structure used in previous studies in the SVP system to automate the certification procedure of the grid support functions. This new structure simplifies the introduction of a new test-logic related to new standards for certifying the above-mentioned functions. Additionally, data post-processing methods were created to allow the user to evaluate the results in a faster and more efficient way.

Finally, since the Python Test Scripts were placed on the SVP Open-Source repository, collaboration and future development are encouraged to optimize and improve the methodology proposed.

References

[1] IEA, "Solar pv." https://www.iea.org/reports/solar-pv, 2021. (Accessed on 18/04/2022).

[2] N. Ninad, E. Apablaza, M. Bui, J. Johnson, S. Gonzalez, W. Son, C. Cho, J. Hashimoto, K. Otani, R. Bründlinger, R. Ablinger, C. Messner, C. Seitl, Z. Miletic, T. Moore, R. Heidari, I. Temez, F. Baumgartner, F. Carigiet, and J. Kumar K, "Development and evaluation of open-source ieee 1547.1 test scripts for improved solar integration," 09 2019.

[3] "Requirements for generating plants to be connected in parallel with distribution networks - Part 10 Tests demonstrating compliance of units," *prEN 50549-10:2022*, 2022.

[4] J. Johnson, R. Ablinger, R. Bründlinger, B. Fox, and J. Flicker, "Design and evaluation of sunspec-compliant smart grid controller with an automated hardware-in-the-loop testbed," *Technology and Economics of Smart Grids and Sustainable Energy*, vol. 2, 09 2017.

[5] J. Johnson, "Collaborative development of automated advanced interoperability certification test protocols for pv smart grid integration," 09 2014.

[6] M. F. Akorede, H. Hizam, and E. Pouresmaeil, "Distributed energy resources and benefits to the environment," *Renewable and Sustainable Energy Reviews*, vol. 14, no. 2, pp. 724–734, 2010.

[7] J. . Choi and D. . Won, "Advanced active power control considering the characteristics of distributed energy resources in microgrid," *Journal of Electrical Engineering and Technology*, vol. 11, no. 5, pp. 1100–1107, 2016.

[8] S. A. Kalogirou, "Chapter nine - photovoltaic systems," in *Solar Energy Engineering* (S. A. Kalogirou, ed.), pp. 469–519, Boston: Academic Press, 2009.

[9] Z. Gao and K. Sun, *DC–AC inverters*, pp. 354–381. 12 2016.

[10] R. Bründlinger, Z. Miletic, and R. Ablinger, "Ait smart grid converter(sgc) controller featuring sunspec protocol support utilizing hardware-in-the-loop (hil) technology," 09 2016.

[11] N. R. Darghouth, G. L. Barbose, and R. H. Wiser, "The potential impact of increased renewable energy penetrations on electricity bill savings from residential photovoltaic systems," in *World Renewable Energy Forum, WREF 2012, Including World Renewable Energy Congress XII and Colorado Renewable Energy Society (CRES) Annual Conferen*, vol. 4, pp. 2748–2755, 2012.

[12] I. Abdelmotteleb, T. Gómez, and J. P. Chaves-Avila, "Benefits of pv inverter volt-var control on distribution network operation," in *2017 IEEE Manchester PowerTech*, pp. 1–6, 2017.

[13] M. Kraiczy, L. Fakhri, T. Stetz, and M. Braun, "Do it locally: Local voltage support by distributed generation – a management summary," *Report IEA-PVPS T14-08:2017*, 01 2017.

[14] T. Stetz, F. Marten, and M. Braun, "Improved low voltage grid-integration of photovoltaic systems in germany," *IEEE Transactions on Sustainable Energy*, vol. 4, no. 2, pp. 534–542, 2013.

[15] "Requirements for generating plants to be connected in parallel with distribution networks - Part 1: Connection to a LV distribution network - Generating plants up to and including Type B," *EN50549-1:2019*, 2019.

[16] "Requirements for generating plants to be connected in parallel with distribution networks - Part 2: Connection to a MV distribution network - Generating plants up to and including Type B," *EN50549-1:2019*, 2019.

[17] P. Sarhadi and S. Yousefpour, "State of the art: hardware in the loop modeling and simulation with its applications in design, development and implementation of system and control software," *International Journal of Dynamics and Control*, vol. 3, 01 2014.

[18] M. Bacic, "On hardware-in-the-loop simulation," in *Proceedings of the 44th IEEE Conference on Decision and Control*, pp. 3194–3198, 2005.

[19] M. D. Omar Faruque, T. Strasser, G. Lauss, V. Jalili-Marandi, P. Forsyth, C. Dufour, V. Dinavahi, A. Monti, P. Kotsampopoulos, J. A. Martinez, K. Strunz, M. Saeedifard, X. Wang, D. Shearer, and M. Paolone, "Real-time simulation technologies for power systems design, testing, and analysis," *IEEE Power and Energy Technology Systems Journal*, vol. 2, no. 2, pp. 63–73, 2015.

[20] SunspecAlliance, "Sunspec svp." https://sunspec.org/svp-lab/. (Accessed on 01/06/2022).

Annex A: prEN50549-10 - Important Terms and definitions

The following are a series of definitions that can be found in the prEN50549-10 considered as essential to carry out all the tests proposed in this study.

- **Steady state:** state of a system at which all state and output variables remain constant in time while all input variables are constant. In this way, when performing the tests under periodic conditions will be considered as Steady state.
- **Maximum reactive power - Overexcited** ($Q_{max-over}$)**:** maximum continuous overexcited reactive power, measured in a 10 minutes average, which the PV inverter can exchange.
- **Maximum reactive power - Underexcited** ($Q_{max-under}$)**:** maximum continuous underexcited reactive power, measured in a 10 minutes average, which which the PV inverter can exchange.
- **Root-mean-square value, RMS value or Quadratic mean:** is a quantity representing the quantities in a finite set or in an interval,
  - for n quantities x_1, $x_2 \ldots x_n$, by the positive square root of the mean value of their squares, as shown in the Eq. 4.

$$X_q = \left[\frac{1}{n}\left(x_1^2 + x_2^2 + \cdots + x_n^2\right)\right]^{\frac{1}{2}} \tag{4}$$

  - for a quantity x depending on a variable t, by the positive square root of the mean value of the square of the quantity taken over a given interval (t_0,t_0+T) of a variable, as shown the Eq. 5.

$$X_q = \left(\frac{1}{T}\int_{t_0}^{t_0+T}(x(t))^2 dt\right)^{\frac{1}{2}} \tag{5}$$

- **Positive sequence value:** for a three-phase system with phases $L1$, $L2$ and $L3$, the symmetrical sinusoidal three-phase set of voltages or currents having frequency equal to the fundamental frequency is defined by the following complex mathematical expression shown in Eq. 6, where $\underline{a} = e^{j2\pi/3}$ is the 120 degree operator, and X_{L1}, X_{L2} and X_{L3} are the complex expressions of the fundamental frequency phase quantities

concerned, that is, current or voltage phasors.

$$\underline{X}_1 = \frac{1}{3}\left(\underline{X}_{\mathrm{L1}} + \underline{\mathrm{a}}\underline{X}_{\mathrm{L2}} + \underline{\mathrm{a}}^2\underline{X}_{\mathrm{L3}}\right) \tag{6}$$

Annex B: EN50549-10 Testing conditions

Test of the real generating unit control unit in a simulated environment denoted as "Controller-Hardware-in-the-loop" (CHIL), is defined by all following conditions according to the section 4.2.12 section of prEN50549-10:

- The power components of the generating unit, the primary energy source and the distribution grid, are replaced by simulation models running on a real-time computing system.
- The real control unit of the generating unit is connected through analogue, digital and communication interfaces to the virtual representation of the physical system.
- The firmware of the control unit of the generating unit is not changed.

The simulation models need to be validated, based on measured data from tests performed on the complete generating unit or electrical generating system. The model validation process is currently under consideration. However, the Standard establishes that a model validated according to alternative procedure described in other recognized standard can be adopted if the model shows similar or higher fidelity and upon agreement with the relevant parties involved in the conformity process.

Annex C: AIT Smart Grid Converter Data-sheet

	ASGC 34.5TL-PV-3P4W	ASGC 34.5TL-EES-4P4W
DC side		
DC max. input voltage	1000 V	900 V
DC full power MPPT/BATT voltage range (PF=1)	570 - 850 V	570 - 850 V
DC operating voltage range at nominal AC voltage	570 - 950 V	570 - 850 V
DC start voltage at nominal AC voltage	600 V	570 V
DC max. array short circuit current	75 A	75 A
DC max. PV/BATT operating current	60 A	60 A
Number of MPPT / max. number of inputs	1 / 2	1 / 2
DC terminal	Screw clamp terminal, AL or CU type cable	Screw clamp terminal, AL or CU type cable
AC side		
AC max. output power	34.5 kW	34.5 kW
AC max. continuous apparent power (at nominal AC voltage)	34.5 kVA	34.5 kVA
AC nominal output voltage / AC operating voltage range	3~NPE 380 V / 220 V or 3~NPE 400V / 230V +/-20%	3~NPE 380V / 220V or 3~NPE 400V / 230V +/-20%
AC nominal frequency / Frequency range	50 Hz and 60 Hz / 45-55 Hz and 55-65 Hz	50 Hz and 60 Hz / 45-55 Hz and 55-65 Hz
AC max. continuous output current	50 A	50 A
AC output current surge capability	N/A	105 A / 60 sec
Power factor range	0 to 1.0 over/under excited	0 to 1.0 over/under excited
THD at max. power	< 3%	< 3%
AC terminal	3 Phase 4 Wire 4-pos. + PE, Socket mating Plug included	3 Phase & Neutral 4 Wire 4-pos. + PE, Socket mating Plug included
AC disconnect	Not included	Not Included
AC connection	3 wire grounded WYE and ungrounded DELTA	4 wire grounded WYE
General data		
Peak efficiency / Weighted efficiency EU/CEC	98. 7% / 98. 2%	98. 7% / 98. 2%
Enclosure type protection class (electronics/mags)	IP 65 / IP 20	IP65 / IP 20
Weight	40 kg./ 88 lbs	45 kg./ 99 lbs.
Dimension (H x W x D)	800 x 600 x 250 cm/ 31.5 x 23.6 x 9.8 in	800 x 600 x 250 cm/ 31.5 x 23.6 x 9.8 in
Ambient air temperature for operation	-25°C to 60°C / -13°F to 140°F	-25°C to 60°C / -13°F to 140°F
Max. operating altitude	2000 m / 13123 ft	2000 m / 13123 ft
Relative humidity %	0...100% non-condensing	0...100% non-condensing
Audible noise	35 dBA +/- 3 dBA	35 dBA +/- 3 dBA
User interface and communications		
User interface	CLI / Widgets based custom UI	CLI / Widgets based custom UI
Communications	ModBus TCP, IEC61850, SunSpec	ModBus TCP, IEC61850, SunSpec
Regulatory approvals		
Safety & EMC	IEC 62477-1, IEC 62109 IEC 61000-6-2, IEC 61000-6-3	IEC 62477-1, IEC 62109 IEC 61000-6-2, IEC 61000-6-3
Grid code compliance	VDE-AR-N4110, VDE-AR-N 4105, IEEE1547a, UL1741-SA	VDE-AR-N4110, VDE-AR-N 4105, UL1741-SA

Figure 32: AIT Smart Grid Converter Data-sheet.

Annex D: Typhoon HIL 402 Data-sheet

Processor		Up to 4 cores
Analog I/O	Channels	16 inputs / 16 outputs
	Resolution	16 bit
	Voltage range	± 10 V
	Sample rate	1 MSPS
	Protection	± 24 V tolerant, ESD protection
	Connector	DIN 41612, type C, 96 pin male connector
Digital I/O	Channels	32 inputs / 32 outputs
	Threshold voltages (DI)	$V_{IL(max)} = 0.8$ V; $V_{IH(min)} = 2.0$ V
	Threshold voltages (DO)	$V_{OL(max)} = 0.2$ V; $V_{OH(min)} = 4.8$ V
	Input resistance	10 kΩ
	Protection	± 24 V tolerant, ESD protection
	Connector	DIN 41612, type C, 96 pin male connector
Externally available power supply	± 5 V analog	up to 1 A, resettable protection
	± 12 V analog	up to 0.5 A, resettable protection
	3.3 V digital	up to 1 A, resettable protection
	5 V digital	up to 1 A, resettable protection
Connectivity	USB	2.0 high speed, B-type connector
	Ethernet	RJ45 connector
Compatibility	HIL DSP interface	
	HIL uGrid DSP interface	
	HIL Breakout board	
	HIL dSpace interface board	
Power supply	External	100 - 250 VAC, ≥ 60 W

Figure 33: Typhoon HIL 402 Data-sheet.

Annex E: Test result for different irradiances

Figure 34: Test result for different irradiances: Voltage related control mode for reactive power (Steady state behaviour) - Setting (a).